Separation of Series Resistance and Space Charge Region Recombination in Crystalline Silicon Solar Cells From Dark and Illuminated Current–Voltage Characteristics

Johannes Greulich, Markus Glatthaar, and Stefan Rein

***Abstract*—The measurement of current–voltage *(J–V)* characteristics is one of the most straightforward methods for the characterization of solar cells. Consequently, an accurate knowledge of its meaning is of high relevance for the comprehension and technological feedback of these devices. The internal series resistance is one limiting parameter of the fill factor and the efficiency of these devices. A second limiting parameter is the p-n junction space charge region recombination. In this paper, we present a method to determine the lumped series resistance by combining the *J–V* characteristics in the dark and under 1-sun illumination. As a first approximation, the lumped series resistance under illuminated conditions is used for the dark *J–V* characteristic at small currents. Based on this, we present a method to quantify resistive losses and space charge region recombination only from the dark and illuminated *J–V* curves so that a simple separation of both losses becomes possible with all inline cell testers.**

***Index Terms*—Fill factor, recombination, series resistance, solar cell.**

I. Introduction

VARIOUS types of losses limit the energy conversion efficiency of a solar cell and influence the shape of its current–voltage (*J–V*) characteristics in a specific way. The reliable separation of resistive losses from losses caused by p-n junction space charge region (scr) recombination, i.e., diode-like recombination current with ideality larger than 1, is a challenge since both mainly influence the maximum power point (mpp) and the fill factor *FF* of the device [1]. The curve fit of the two-diode model fails because the assumption of a lumped series resistance cannot account for the lateral variations of the quasi-Fermi potential within the solar cell. However, the analysis of the fill factors *FF* of the illuminated *J–V* curve, *pFF* [2] of the suns-V_{oc} curve and FF_0 [3] of the ideal *J–V* curve, respectively, is capable of separating both losses if the series resistance of the device is not very large and if the shunt resistance is larger than approximately 3 k$\Omega\cdot$cm^2, which is usually fulfilled in industrial-type crystalline silicon solar cells [4]. The quantification of the lumped series resistance from the dark and the 1-sun-illuminated *J–V* characteristics is also possible with other methods [5], [6]. We present a different method to quantify resistive losses that circumvents the disadvantages of these methods. We further use the series resistance to determine scr recombination based on the *J–V* characteristics in the dark and under 1-sun illumination. Using only these two *J–V* curves has the advantage that the measurement of the dark and illuminated curves is rather simple and, therefore, is available at all current inline cell testers.

In the first part of this paper, we present the new method for the separation of resistive losses and losses caused by scr recombination and apply it to simulated *J–V* characteristics. In the second part, we exemplarily apply the new method and the reference techniques to measured *J–V* curves of intentionally damaged solar cells and analyze the impact of injection-dependent bulk and surface recombination on the new method.

II. Theory and Simulation

A. Determination of the Lumped Series Resistance

There are many methods for the quantification of resistive losses [7], where the lumped series resistance R_s is used as characteristic parameter. In this section, we first review two methods to determine R_s based on the dark and illuminated *J–V* curves and then derive a new expression.

The method by Aberle *et al*. [5] starts with the mpp of the 1-sun-illuminated *J–V* curve that is affected by R_s and the dark *J–V* curve which they assume to be unaffected by R_s for small currents $J = |J_{\mathrm{sc}} - J_{\mathrm{mpp}}|$. They derive the following expression for the lumped series resistance:

$$R_{s,\mathrm{Aberle}} = \frac{\Delta V_{\mathrm{illum}}}{|J_{\mathrm{mpp}}|} = \frac{V_{\mathrm{dark}} - V_{\mathrm{mpp}}}{|J_{\mathrm{mpp}}|} \quad (1)$$

Manuscript received November 21, 2011; accepted February 17, 2012. Date of publication April 18, 2012; date of current version June 18, 2012. This work was supported in part by the German Ministry for Environment, Nature Conservation and Nuclear Safety, within the framework of the project QUASSIM (0325132A). The work of J. Greulich was supported by a scholarship from the German Federal Environmental Foundation [Deutsche Bundesstiftung Umwelt (DBU)].

J. Greulich is with the Fraunhofer Institute for Solar Energy Systems, 79110 Freiburg, Germany, and also with the Material Research Center, University of Freiburg, 79110 Freiburg, Germany (e-mail: johannes.greulich@ise.fraunhofer.de).

M. Glatthaar and S. Rein are with the Fraunhofer Institute for Solar Energy Systems, 79110 Freiburg, Germany (e-mail: markus.glatthaar@ise.fraunhofer.de; stefan.rein@ise.fraunhofer.de).

Color versions of one or more of the figures in this paper are available online at http://ieeexplore.ieee.org.

Digital Object Identifier 10.1109/JPHOTOV.2012.2189370

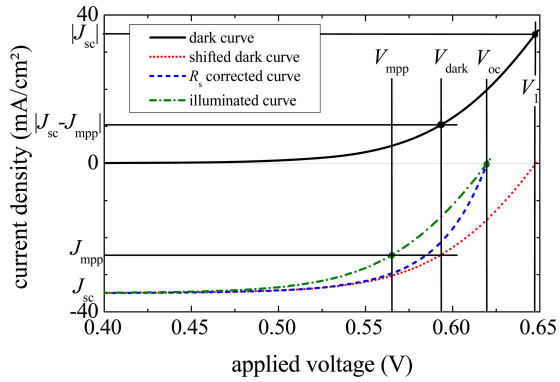

Fig. 1. Relevant *J–V* characteristics illustrating the evaluation method. The lumped series resistance is directly calculated from the voltage difference between the shifted dark *J–V* characteristic and the illuminated *J–V* characteristic. After a series resistance correction, the dark pseudo fill factor is calculated from the shifted and corrected dark *J–V* curve.

where $V_{\mathrm{dark}} = V(J = |J_{\mathrm{sc}} - J_{\mathrm{mpp}}|)$ is the voltage of the dark *J–V* curve with a current equal to $|J_{\mathrm{sc}} - J_{\mathrm{mpp}}|$ (see Fig. 1).

This is an appealingly simple expression, but Dicker showed that the assumption of a not R_s-affected dark *J–V* curve does not hold [6]. Therefore, in contrast to Aberle, Dicker uses the more complex expression for the lumped series resistance

$$R_{s,\mathrm{Dicker}} = \frac{V_{\mathrm{dark}} - \Delta V_{\mathrm{dark,Dicker}} - V_{\mathrm{mpp}}}{|J_{\mathrm{mpp}}|} = \frac{V_{\mathrm{dark}} - V_{\mathrm{mpp}}}{|J_{\mathrm{mpp}}|} - \frac{|J_{\mathrm{sc}} - J_{\mathrm{mpp}}| \cdot \frac{V_1 - V_{\mathrm{oc}}}{|J_{\mathrm{sc}}|}}{|J_{\mathrm{mpp}}|}. \quad (2)$$

Here, V_1 denotes the voltage of the dark characteristic at $J = |J_{\mathrm{sc}}|$ (see Fig. 1). Therefore, Dicker needs to measure the dark *J–V* curve up to relatively high currents $J = |J_{\mathrm{sc}}|$, which results in a relatively large absolute measurement error, which is in particular important at small currents $J = |J_{\mathrm{sc}} - J_{\mathrm{mpp}}|$. Furthermore, at such high currents under dark conditions, the current paths may differ more from the current paths under illumination than at smaller dark currents. Finally, Dicker uses V_{oc} and V_1 to calculate the lumped series resistance at a significantly lower voltage V_{mpp}, which is a combination of different injection conditions. This is a questionable approach for highly injection-dependent devices as solar cells with passivation at the rear surface [8] and can result in inaccurate values of the lumped series resistance.

The method that we propose is similar to both methods. As Aberle, we determine R_s from the dark and illuminated current voltage curves at mpp. As Dicker, we assume that the dark *J–V* curve is affected by a series resistance. However, unlike Dicker, we assume that the dark *J–V* curve is influenced by the same lumped series resistance as the illuminated *J–V* curve as a first approximation. This constitutes a simplification since the lumped R_s in the dark and under illumination generally are different. Since the voltage drop at $J = |J_{\mathrm{sc}} - J_{\mathrm{mpp}}|$ of the dark *J–V* curve is rather small (typically roughly 2 mV) compared with the voltage drop at $J = J_{\mathrm{mpp}}$ of the illuminated *J–V* curve (roughly 25 mV), the error caused by this simplification is small. This series resistance leads to a voltage difference of the dark *J–V* curve at $V(J = |J_{\mathrm{sc}} - J_{\mathrm{mpp}}|)$ between the applied voltage V_{applied} and the junction voltage V_{junction} larger than zero:

$$\Delta V_{\mathrm{dark}} = V_{\mathrm{applied}} - V_{\mathrm{junction}} = |J_{\mathrm{sc}} - J_{\mathrm{mpp}}| \cdot R \quad (3)$$

where ΔV_{dark} is typically in the milivolt range (e.g., 2.5 mA/cm^2· 0.8 Ω·cm^2 = 2.0 mV). This indicates that the device can be treated as an equipotential surface since the lateral voltage variation ΔV_{dark} within the device is much smaller than the thermal voltage $V_t(25\ ^\circ\mathrm{C}) \approx 25.7$ mV. Therefore, the assumption of a lumped series resistance is justified as well. As Aberle and Dicker, we assume that the series resistance induces a voltage drop of the illuminated characteristic smaller than zero, since $J_{\mathrm{mpp}} < 0$:

$$\Delta V_{\mathrm{illum}} = J_{\mathrm{mpp}} \cdot R. \quad (4)$$

$\Delta V_{\mathrm{illum}}$ is typically in the range of the thermal voltage V_t (e.g., 33 mA/cm^2 · 0.8 Ω·cm^2 = 26.4 mV). Therefore, the device cannot be treated as equipotential surface, and the distributed series resistance is taken into account in the following simulations. However, the lumped series resistance can be regarded as a figure of merit. Adding both voltage drops yields the total voltage difference ΔV that is in contrast with ΔV_{dark} and $\Delta V_{\mathrm{illum}}$ a measurable quantity ($\Delta V = V_{\mathrm{dark}} - V_{\mathrm{mpp}}$; see Fig. 1). By dividing ΔV by the total difference of the current densities $\Delta J = |J_{\mathrm{sc}}|$, we obtain

$$R_{s,\mathrm{new}} = \frac{\Delta V}{\Delta J} = \frac{\Delta V_{\mathrm{illum}} + \Delta V_{\mathrm{dark}}}{|J_{\mathrm{mpp}}| + |J_{\mathrm{sc}} - J_{\mathrm{mpp}}|} = \frac{V_{\mathrm{dark}} - V_{\mathrm{mpp}}}{|J_{\mathrm{sc}}|} \quad (5)$$

as expression for the lumped series resistance. It is as simple as Aberle's expression and accounts for the voltage drop at R_s of the dark *J–V* curve. As a first-order approximation, it is assumed that R_s of the dark and illuminated *J–V* characteristics is identical. The expression does not depend on those parts of the dark *J–V* curve with relatively high currents $J = J_{\mathrm{sc}}$ and, hence, allows for a more precise measurement of the *J–V* curve at $J = |J_{\mathrm{sc}} - J_{\mathrm{mpp}}|$ because an adapted sensing resistor can be chosen. Furthermore, (5) reduces the spread of operating voltages (no measurements at $V \geq V_{\mathrm{oc}}$). The charge carrier lifetime and the surface recombination velocity can be injection dependent, in particular, for solar cells with passivated rear side [8]. Since the injection level depends on the junction voltage V_{pn} and the illumination conditions, the reduced spread of operating voltages reduces possible injection dependences. Besides, differences concerning the current paths are reduced. The remaining dependence of the injection level on the illumination conditions still can lead to artificial effects in the case of injection-dependent devices when combining measurements under illumination and dark conditions as in (1), (2), and (5). See Section III-B for more details.

B. Separation of Resistive Losses and Space Charge Region Recombination

As reference method to quantify resistive losses and scr recombination, we choose the difference between the pseudo fill

TABLE I
SIMULATION PARAMETERS

Parameter	Values			Units	Explication
$J_{01,\mathrm{met}}$	0.6	2	4	fA/cm²	Saturation current of the first diode, metalized area
$J_{01,\mathrm{n\text{-}met}}$	0.6	1	2	fA/cm²	Saturation current of the first diode, not metalized area
$J_{02,\mathrm{met}}$	5	50	200	nA/cm²	Saturation current of the second diode, metalized area
$J_{02,\mathrm{n\text{-}met}}$	5	30	50	nA/cm²	Saturation current of the second diode, not metalized area
$n_{2,\mathrm{met}}$	2	3.5			Ideality factor of the second diode, metalized area
$n_{2,\mathrm{n\text{-}met}}$	2	3.5			Ideality factor of the second diode, not metalized area
r_{C}	4	10		mΩcm²	Metal-semiconductor contact resistance
R_{sh}	65	80		Ω	Emitter sheet resistance
R_{f}	20	50		Ω/m	Finger resistance

List of varied input parameters and of the used values used for the simulation. A full factorial design of experiment is applied yielding 2592 combinations.

factor *pFF* and the fill factor *FF*, which directly relates to the series resistance, and the difference between the ideal fill factor FF_0 and *pFF*, which directly relates to scr recombination and shunt losses. The latter can be neglected if the shunt resistance is larger than approximately 3 kΩ·cm² [4]. The new approach proposed here is to correct the dark *J–V* characteristic for the resistive loss using the lumped series resistance and, subsequently, calculate the pseudo fill factor from the corrected dark *J–V* characteristic, which is rather easy to measure and, therefore, rather widely used, instead of the suns-V_{oc} curve. We suggest calling this approximation the dark pseudo fill factor *dpFF*.

First, we apply the following procedure to the voltage of the dark *J–V* curve in order to correct the voltage drop at the series resistance (cf., Fig. 1):

$$V_i \rightarrow V_i' = V_i - J_i \cdot R_S. \tag{6}$$

Here, V_i and J_i designate the measured voltage and the corresponding current density of the dark *J–V* curve. V_i' designates the corrected voltage. We use the lumped R_s determined with (5), which approximately corresponds to the series resistance of the illuminated *J–V* characteristic. This quantity is generally different from the series resistance of the dark *J–V* curve and serves here only as a first approximation of the latter. As already stated above, errors in R_s cause small errors in V_i' since the correction term $J_i \cdot R_s$ is small (a couple of millivolts) compared with V_i (a couple of hundred millivolts) in the *J–V* regime considered in the following. The use of a lumped R_s in contrast to a distributed resistance is justified because at such small dark currents, only small voltage variations occur and the device can be treated as an equipotential surface. After this correction procedure, *dpFF* is calculated by shifting the corrected dark forward *J–V* curve by $\Delta J = -|J_{\mathrm{sc}}|$ along the current axis from the first into the fourth quadrant. We define *dpFF* as the maximum power $P_{\mathrm{dMPP}} = V_{\mathrm{dMPP}} \cdot J_{\mathrm{dMPP}}$ of this corrected and shifted dark *J–V* curve divided by the open-circuit voltage V_{oc} and the short-circuit current density J_{sc} of the illuminated *J–V* curve

$$dpFF = \frac{P_{\mathrm{dMPP}}}{J_{\mathrm{sc}} \cdot V_{\mathrm{oc}}} = \frac{V_{\mathrm{dMPP}} \cdot J_{\mathrm{dMPP}}}{J_{\mathrm{sc}} \cdot V_{\mathrm{oc}}}. \tag{7}$$

Here, V_{dMPP} and J_{dMPP} denote the voltage and the current density at the mpp of the shifted dark *J–V* curve. Using the open-circuit voltage V_{oc} of the illuminated curve, not of the shifted dark *J–V* curve has two advantages. First, it is not necessary to measure the whole dark *J–V* curve that allows higher accuracy as the sensing resistor can be adapted to small currents. Second, using the measured open-circuit voltage avoids possible errors induced by the approximation of the series resistance as a lumped parameter and/or the curve correction (6).

As mentioned previously, the minority carrier density *n(z)* depends not only on the junction voltage V_{pn}, but also on the illumination conditions. Therefore, injection-dependent minority carrier lifetimes and injection-dependent surface recombination velocities can lead to artificial effects in the methods based on the *FF* of the 1 sun *J–V* curve, on the *pFF* of the suns-V_{oc} curve, and on the *dpFF* of the dark *J–V* curve.

In order to evaluate the methods for the determination of series resistance and scr recombination, we use a quasi-2-D simulation tool to simulate the *J–V* curves of the solar cells [4]. This model accounts for different distributed contributions to the series resistance, for lateral variation of recombination mechanisms [9] and for shading by the front metallization. Within this model, the local *J–V* curve is approximated with the two-diode model. The local cell parameters J_{sc}, J_{01} (dark saturation current density of the first diode with ideality $n_1 = 1$), J_{02} (dark saturation current density of the second diode with ideality $n_2 > 1$, representing scr recombination), and n_2 are independently set to different values 1) in the cell area covered by the front-side metallization (fingers and bus bars) and 2) in the nonmetalized cell area. We use this model to generate artificial measurement data as a basis for the following analysis by varying the parameters typically met in industrial silicon solar cells given in Table I. A full factorial design of (artificial) experiment is applied, yielding 2592 different parameter combinations. For each parameter combination, all relevant *J–V* curves and parameters are calculated. In order to quantify the influence of the scr recombination, first, the efficiency η_i without J_{02} (i.e., with $J_{02} = 0$) and then the efficiency η_f with J_{02}, as given in Table I, are calculated. The difference $\Delta\eta = \eta_i - \eta_f$ representing losses due to scr recombination J_{02} is used as a reference for the following comparison of methods for the separation of resistive losses and scr recombination that are applied to the artificial measurement data.

We apply Aberle's, Dicker's, and our method to determine R_s (see Fig. 2). The deviation of Aberle's method from the other methods increases from 0.02 to 0.08 Ω·cm² as R_s increases from 0.4 to 1.0 Ω·cm². We attribute this to Aberle's unjustified assumption that the dark *J–V* characteristic is unaffected by R_s. Dicker's method and our new method yield similar results, our new method yielding less than 0.02 Ω·cm² smaller values.

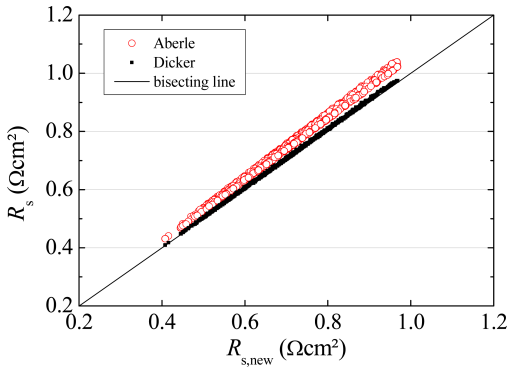

Fig. 2. Comparison of Aberle's and Dicker's method with the new one for series resistance determination shows that Aberle yields the highest values with increasing deviation from the other methods. This is due to the disregard of the influence of the series resistance on the dark current voltage curve. Aberle's and the new method agree closely due to similar assumptions.

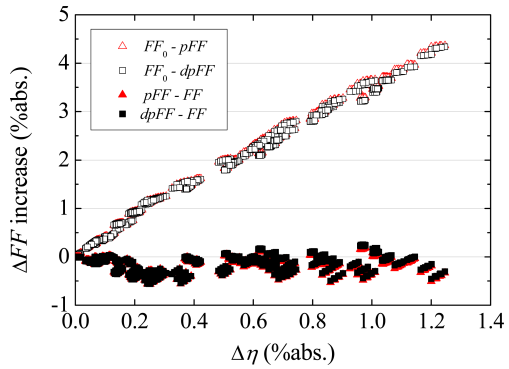

Fig. 3. Fill factor differences $FF_0 - pFF$ and $FF_0 - dpFF$ (empty symbols) increase almost linearly with increasing scr recombination loss $\Delta\eta$ when applied to the simulated data. The fill factor differences $pFF - FF$ and $dpFF - FF$ (filled symbols) related to series resistance losses do not increase with $\Delta\eta$.

The fill factor differences $FF_0 - pFF$ and $FF_0 - dpFF$ linearly correlate with the scr recombination loss $\Delta\eta$ as shown in Fig. 3. As expected the differences $pFF - FF$ and $dpFF - FF$ related to resistive losses do not increase as the scr recombination loss changes. The use of $dpFF$ instead of pFF systematically yields 0.01 %abs. smaller values, which lies within the scatter of the data in Fig. 1. We conclude from these simulations that combined with FF and FF_0, the newly introduced $dpFF$ can be used to determine separately fill factor losses caused by the series resistance and those caused by scr recombination with about the same accuracy as the pFF from the suns-V_{oc} curve. Thus, a simple loss analysis based only on the dark and illuminated J–V characteristics is possible.

III. Experimental Details

A. Application to Intentionally Damaged Solar Cells

In order to provide proof that the separate quantification of the losses related to the series resistance and to scr recombination is possible with the methods presented and in order to gain more confidence, we apply the methods based on (5) and (7) to J–V characteristics of intentionally damaged solar cells produced and measured in an industrial environment. We processed 18 solar cells on p-type Czochralski silicon wafers with a pseudosquare format of 156 mm × 156 mm using a standard industrial process with aluminum back surface field (BSF). After light soaking for stabilizing the boron–oxygen defect, the dark and 1-sun illuminated J–V characteristics and the suns-V_{oc} curve are measured in the initial state. From these curves, we determine the conversion efficiency η, FF_0, pFF, FF, R_s after Aberle, Dicker, and after our procedure as well as $dpFF$. We then split the 18 cells into four groups. In order to change only the scr recombination keeping all other cell parameters constant, we use the laser edge isolation process again to generate grooves in between all front metallization fingers (see Fig. 4), the total groove length varying between 2 × 156 and 12 × 156 mm. After this laser process, we measure and evaluate the current voltage curves a second time in the final state in the same manner as before.

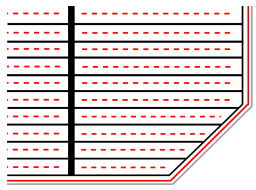

Fig. 4. Details of the front side of a solar cell. Between the metallization (black continuous lines), the laser grooves (red dashed lines) are sketched. Also visible are the wafer edges (gray continuous lines) and the laser edge isolation grooves (red continuous lines).

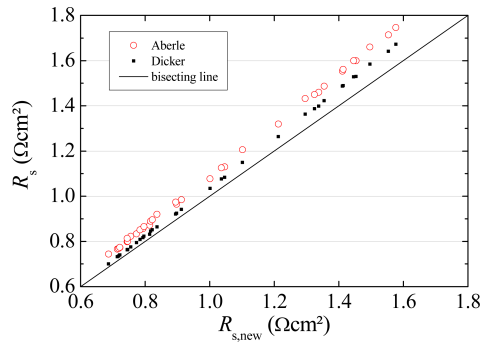

Fig. 5. Similar to the simulation, the measured series resistance as determined with Dicker's method and with (5) ("$R_{s,new}$") correlate closely, while Aberle's method yields systematically the highest values.

As expected, J_{sc}, V_{oc}, R_s, and R_p are almost unaffected by the laser grooving. R_p is on a high level above 10 kΩ·cm² for all cells before and after laser scribing. Aberle's R_s-method yields approximately 0.08 Ω·cm², Dicker's method 0.03 Ω·cm² higher values than our method (see Fig. 5). This confirms the findings of the simulation. The high values of the series resistance of some solar cells with $R_s > 1$ Ω·cm² are caused by suboptimal contact formation conditions.

As before, we choose the efficiency difference $\Delta\eta = \eta_i - \eta_f$ between the first measurement in the initial state and the second measurement in the final state as reference, η_i representing the laser damage-free case. In order to eliminate any offsets, we consider the increase of the fill factor differences $pFF - FF$, $dpFF - FF$ and $FF_0 - pFF$, $FF_0 - dpFF$ between the first and the second measurement (see Fig. 6).

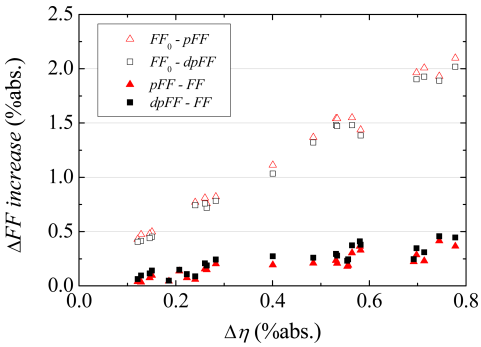

Fig. 6. Similar to the simulation, the measured fill factor differences $FF_0 - pFF$ and $FF_0 - dpFF$ increase almost linearly with increasing efficiency loss $\Delta\eta$. The fill factor differences $pFF - FF$ and $dpFF - FF$ related to series resistance losses increase only slightly with $\Delta\eta$.

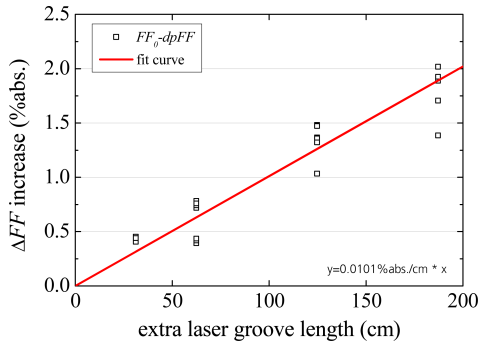

Fig. 7. Increase of the scr recombination losses $\Delta FF = FF_0 - dpFF$ scales approximately linear with the extra laser groove length. The linear curve fit yields a proportionality factor of $m = 0.0101$ %abs./cm.

In contrast to the simulations, $pFF - FF$ and $dpFF - FF$ slightly increase by less than 0.5 %abs. with increasing $\Delta\eta$, which may be attributed to a small misalignment of the laser grooves in between the front-side metallization which would increase the ohmic losses in the emitter. Another reason for the slight increase of $pFF - FF$ and $dpFF - FF$ may be that the additional recombination current induced by the laser groves is limited to the disturbed regions between the fingers as shown by Steingrube *et al.* [10] in combination with different local junction voltages at the (pseudo) mpps of the illuminated, suns-V_{oc}, and dark J–V characteristics. For a given terminal voltage $V_{terminal}$ at the (pseudo) mpp, the local p-n junction voltage V_{pn} at the disturbed regions is the highest for the illuminated J–V curve, medium for the suns V_{oc} curve, and the lowest for the dark J–V curve. The disturbed regions, therefore, contribute rather strongly to the total recombination current for the illuminated and rather slightly for the dark case. This causes a rather small FF, a medium pFF, and a slightly larger $dpFF$, which qualitatively can explain the behavior of $pFF - FF$ and $dpFF - FF$ in Fig. 6. This effect is specific to the lateral distribution of the laser grooves in the present experiment (see Fig. 4). In solar cells without laser grooves, there is higher recombination at the metallization fingers, not between them, as has been taken into account in the simulations. In this case, we expect qualitatively the opposite behavior of $pFF - FF$ and $dpFF - FF$.

As expected, both $FF_0 - pFF$ and $FF_0 - dpFF$ increase linearly by up to approximately 2 %abs. with increasing $\Delta\eta$. The use of $dpFF$ instead of pFF of the suns-V_{oc} curve yields approximately 0.1 % lower values, which can qualitatively be explained again by the higher junction voltage at the disturbed regions under open-circuit conditions compared with the dark conditions. Another reason for this small deviation may be the fine-tuning of the J–V measurement tool. Anyway, Fig. 6 confirms that the separation of scr recombination and resistive losses is equally well possible with $dpFF$ as with the suns-V_{oc} pFF.

The laser grooving between the fingers can be used to evaluate the laser process, e.g., for edge isolation or ablation of the antireflection coating, independently of the other cell parameters as series resistance and short-circuit current. This is exemplarily done here for the laser edge isolation process. The linear curve fit of the form $y = m{\cdot}x$, where y corresponds to the increase of scr recombination losses $\Delta FF = FF_0 - dpFF$ and x to the extra laser groove length, yields $m = 0.0101$ %abs/cm (see Fig. 7). With no extra laser grooves, only the usual laser edge isolation induces grooves that are approximately $l_0 = 4 \times 15.6$ cm $=$ 62.4 cm long. From the linear curve fit, we conclude for this specific laser edge isolation process and for our cells that the usual edge isolation causes a fill factor loss of approximately $\Delta FF = m{\cdot}l_0 = 0.62$ %abs., which represents roughly half of the total losses $FF_0 - pFF \approx 1.3$ %abs.

B. Injection-Dependent Bulk and Surface Recombination

After applying the methods to J–V curves of solar cells with full-area aluminum BSF, we would like to discuss the impact of injection-dependent bulk lifetime and surface recombination velocity on the methods. Charge carriers can be injected into a solar cell by applying a voltage to its terminals or by shining light onto the cell. Both voltage and illumination influence the charge carrier profile within a solar cell. Raising the p-n junction voltage raises the charge carrier concentration at the junction, whereas for a given p-n junction voltage, the illumination raises the carrier concentration in the volume of the quasi-neutral regions of the device.

In order to investigate the effect of injection-dependent effective lifetimes on the series resistance methods, we compare the series resistance after Dicker (2), after (5), and from three intensities (0.8, 1.0 and 1.2 suns) as described in the international standard IEC 891 [11]. The IEC-method is regarded here as a reference [7], because it relies only on very similar injection conditions and, therefore, is expected to be unaffected by injection-dependent recombination mechanisms. The methods (1), (2), and (5) combine illuminated and dark conditions and, therefore, rely on different injection levels. We apply these three methods to the J–V curves of three groups of solar cells. The first group consists of nine conventional solar cells made of multicrystalline (mc) p-type silicon featuring a full-area aluminum BSF. The second group comprises nine conventional solar cells made of crystalline Czochralski-grown (Cz) p-type silicon in the resistivity range 1.5–2.5 Ω·cm with a full-area aluminum BSF. Eight solar cells making up the third group with a structure similar to the Passivated Emitter and Rear Cell (PERC) concept [12]

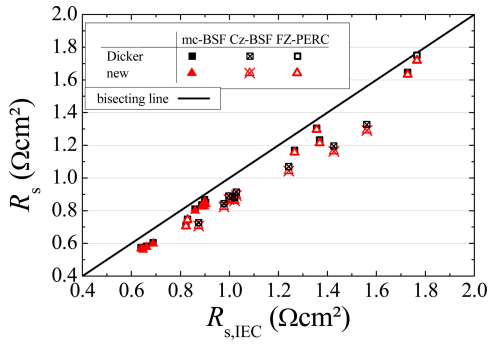

Fig. 8. Methods for the determination of the series resistance after Dicker and the newly proposed method systematically underestimate the series resistance compared with the method based on three intensities as described in the IEC norm both for PERC devices and conventional solar cells with full-area aluminum BSF.

are made of p-type float zone (FZ) silicon with specific resistivity ranging from 0.5 to 4.0 Ω·cm. Their rear side is passivated with SiO_2; the point contact spacing at the rear ranges from 300 to 1500 μm. Fig. 8 shows that the methods by Dicker (2) and the new method (5) agree closely but give systematically lower values than the IEC-method. The Cz-BSF cells show the largest deviation of approximately 0.17 Ω·cm^2. The R_s values of the mc-BSF cells deviate from the IEC-method by approximately 0.06 Ω·cm^2 and by 0.09 Ω·cm^2 for the FZ-PERC devices.

This behavior can be explained as follows. Typically, the surface recombination rate of surfaces coated with SiO_2 and the bulk recombination rate for many types of point defects, e.g., iron or the boron–oxygen defect, in p-type silicon decrease as the injection level increases [7], [13], [14]. Therefore, the junction voltage is higher under illumination than under dark conditions for a given recombination current. This, in turn, leads to the underestimation of $V_{\mathrm{dark}} - V_{\mathrm{mpp}}$ in the series resistance methods (1), (2), and (5) in p-type silicon.

The injection dependence of the bulk lifetime and surface recombination influences not only the determination of the series resistance. The fill factor differences $FF - pFF$ and $FF - dpFF$ tend to underestimate the series resistance losses, and $FF_0 - pFF$ and $FF_0 - dpFF$ tend to overestimate the scr recombination if the bulk and surface recombination decrease as the injection level increases. However, in contrast with the series resistance, there is no reliable reference method in order to quantify this experimentally.

IV. Summary and Conclusion

In order to minimize resistive losses and scr recombination losses, we presented methods for their determination only from the dark and illuminated *J–V* characteristics. We compared these methods with state-of-the-art methods using quasi-2-D simulations and intentionally damaged industrial-type silicon solar cells. The new expression for the series resistance is simpler than the reference by Dicker and agrees with it within an error of 0.03 Ω·cm^2. The newly introduced dark pseudo fill factor is easy to measure and approximates the pseudo fill factor with an accuracy of 0.1 %abs. It serves well to separate resistive and p-n junction scr recombination losses when combined with the fill factor and the ideal or intrinsic fill factor of the device. The impact of injection-dependent bulk and surface recombination, which can cause artifacts in the methods, is discussed and quantified for the series resistance of selected solar cells. Since the methods are based only on the dark and the illuminated current voltage characteristics that are rather easy to measure, it is possible to determine resistive and scr recombination losses separately with all current inline cell testers.

Acknowledgment

The authors would like to thank their colleague A. Krieg for *J–V* measurements and calibration of the cell tester.

References

[1] B. Fischer, P. Fath, and E. Bucher, "Evaluation of solar cell J(V)-measurements with a distributed series resistance model," in *Proc. 16th Eur. Photovoltaic Solar Energy Conf.*, Glasgow, U.K, May 2000, pp. 1365–1368.

[2] R. A. Sinton and A. Cuevas, "A quasi-steady state open circuit voltage method for solar cell characterization," in *Proc. 16th Eur. Photovoltaic Solar Energy Conf.*, Glasgow, U.K, May 2000, pp. 1152–1155.

[3] M. A. Green, *Solar Cells: Operating Principles, Technology and System Applications*. Sydney, N.S.W., Australia: Univ. New South Wales, Dec. 1986, p. 96.

[4] J. Greulich, M. Glatthaar, and S. Rein, "Fill factor analysis of solar cells' current-voltage curves," *Prog. Photovoltaic: Res. Appl.*, vol. 18, no. 7, pp. 511–515, Nov. 2010.

[5] A. G. Aberle, S. R. Wenham, and M. A. Green, "A new method for accurate measurements of the lumped series resistance of solar cells," in *Proc. 23rd IEEE Photovoltaic Spec. Conf.*, Louisville, KY, May 1993, pp. 133–139.

[6] J. Dicker, "Analyse und Simulation von hocheffizienten Silizium-Solarzellenstrukturen für industrielle Fertigungstechniken," Ph.D. dissertation, Dept. Physics, Konstanz Univ., Konstanz, Germany, 2003.

[7] D. Pysch, A. Mette, and S. W. Glunz, "A review and comparison of different methods to determine the series resistance of solar cells," *Sol. Energy Mater. Sol. Cells*, vol. 91, pp. 1698–1706, Nov. 2007.

[8] S. W. Glunz, A. B. Sproul, W. Warta, and W. Wettling, "Injection-level-dependent recombination velocities at the Si-SiO_2 interface for various dopant concentrations," *J. Appl. Phys.*, vol. 75, no. 3, pp. 1611–1615, Feb. 1994.

[9] T. Fellmeth, A. Born, A. Kimmerle, F. Clement, D. Biro, and R. Preu, "Recombination at metal-emitter interfaces of front contact technologies for highly efficient silicon solar cells," *Energy Procedia*, vol. 8, pp. 115–121, Aug. 2011.

[10] S. Steingrube, O. Breitenstein, K. Ramspeck, S. Glunz, A. Schenk, and P. P. Altermatt, "Explanation of commonly observed shunt currents in c-Si solar cells by means of recombination statistics beyond the Shockley-Read-Hall approximation," *J. Appl. Phys*, vol. 110, pp. 014515-1–014515-10, Jul. 2011.

[11] *Procedures for Temperature and Irradiance Corrections to Measured I-V Characteristics of Crystalline Silicon Photovoltaics Devices*, Int. Stand. IEC 891, 1987.

[12] A. W. Blakers, A. Wang, A. M. Milne, J. Zhao, and M. A. Green, "22.8% efficient silicon solar cell," *Appl. Phys. Lett.*, vol. 55, no. 13, pp. 1363–1365, Jul. 1989.

[13] D. Macdonald and L. J. Geerligs, "Recombination activity of interstitial iron and other transition metal point defects in p- and n-type crystalline silicon," *Appl. Phys. Lett.*, vol. 85, no. 10, pp. 4061–4063, Nov. 2004.

[14] S. Rein, *Lifetime Spectroscopy*. Heidelberg, Germany: Springer-Verlag, 2005.

Authors' photographs and biographies not available at the time of publication.